JOURNAL OF MATERIALS SCIENCE 29 (1994) 2507–2512

On the mechanical response of short fibre reinforced polymer composites

L. BIOLZI
Politecnico di Milano, Italy
L. CASTELLANI
Enichem Polimeri, Centro Ricerche, Mantova, Italy
I. PITACCO
Universita' di Udine, Italy

In this paper, a generalized Mori–Tanaka scheme is applied to evaluate the elastic response of short fibre composite materials. Numerical predictions are compared with experimental measurements performed on short fibreglass reinforced thermoplastics with a wide range of fibre concentrations, including the range characteristic of usual industrial applications with non-trivial fibre orientation distribution.

1. Introduction

The central importance of fibre reinforced composite materials in engineering applications is now well-established (cf. for instance, [1]). The effective use of these materials requires a reliable knowledge of their characteristic behaviour, that is, a correct mathematical evaluation of their mechanical properties. The problem of predicting the effective or "overall" macroscopic elastic properties of materials composed of a continuous matrix phase containing embedded inclusions is still an attractive basic subject in mechanics. As these materials are not homogeneous, an estimate of their effective properties necessitates a micro-mechanical analysis that considers the interaction between the fibres and the continuous embedded matrix. When the interaction among fibres is negligible (a dilute condition), Eshelby's method [2] provides the average behaviour of the aggregate. When the fibre concentration level becomes significant, many methods have been proposed to estimate the effective elastic properties of such materials. Among these, the most widely employed are the self-consistent scheme, credited to Budiansky [3] and Hill [4], the Halphin–Tsai equations [5], the differential method [6] and the Mori–Tanaka approach [7].

In the most commonly used version of the self-consistent scheme it is assumed that, when the fibre concentration in the matrix is not negligible, the average strain or stress field in the generic inclusion may be estimated by considering itself as being embedded in a homogeneous medium characterized by the mechanical properties of the composite. The differential method is based on the assumption that the overall composite is a sequence of dilute suspensions. In other words, incremental construction of the composite material by gradual addition of infinitesimal amounts of inclusions occurs. The Halpin–Tsai equations are semi-empirical relationships, based on the self-consistent micro-mechanics solutions developed by Hill. The Mori–Tanaka theory [7] has been proposed in order to evaluate the average internal stress in the matrix of a material containing precipitates with eigenstrain. Critical presentation of several of the prominent theoretical micro-mechanic models can be found, for instance, in [8, 9].

The objective of this work is to compare the numerical estimate of the generalized Mori–Tanaka theory with experimental evaluations of some mechanical properties of short fibre composite specimens and to assess the versatility of this analytical model mimicking the experimental response. A noticeable outcome of this research is that accurate microstructural characterization enables excellent estimation of the overall elastic properties of the material.

2. Generalized Mori–Tanaka theory

Consider a perfectly biphase composite aggregate with far field homogeneous conditions that produce a stress–strain field. An overall or effective (fourth-order) elastic tensor, $\mathscr{C}$, is defined as:

$$\bar{\sigma} = \mathscr{C}\bar{\varepsilon} \tag{1}$$

where $\bar{\sigma}$ and $\bar{\varepsilon}$ represent the average stress–strain field, respectively, related to the property tensors of the matrix $\mathscr{C}^m$ and the inclusions $\mathscr{C}^i$ (cf. [10]) as follows:

$$\bar{\sigma} = \alpha^m \mathscr{C}^m \bar{\varepsilon}^m + \sum_i \alpha^i \mathscr{C}^i \bar{\varepsilon}^i \tag{2}$$

with α^m and α^i being the volume fraction of the matrix, m, and the inclusion, i, respectively. The fundamental assumption of the Mori–Tanaka theory [11] regards the average strain field in the generic inclusion, such that:

$$\bar{\varepsilon}^i = \mathscr{T}(g^i, a^i)\bar{\varepsilon}^m \tag{3}$$

0022–2461

where $\mathscr{T}(g^i, a^i)$ is the so-called Wu's tensor, which is a fourth-order tensor function of the fibre orientation [12], defined in three-dimensional Euler space by the three values g^i, and in the two-dimensional aspect ratio space by the two values a^i. The inclusions are supposed to be of ellipsoidal shape, where d_1^i, d_2^i, d_3^i are principal diameters ($d_1^i \leq d_2^i \leq d_3^i$). The aspect ratios are defined as follows:

$$a_1^i = d_1^i/d_3^i, \quad a_2^i = d_2^i/d_3^i \tag{4}$$

The so-called Euler angle, g^i, will be used to define the fibre orientation with respect to a fixed frame. If $\mathscr{T}'(a^i)$ denotes Wu's tensor in the fibre adherent frame, the tensor $\mathscr{T}(g^i, a^i)$ admits the following decomposition:

$$\mathscr{T}(g^i, a^i) = \mathscr{R}(g^i)\,\mathscr{T}'(a^i) \tag{5}$$

or, in components:

$$\mathscr{T}_{i_1 i_2 i_3 i_4} = \mathscr{R}_{i_1 i_2 i_3 i_4 j_1 j_2 j_3 j_4}\,\mathscr{T}' \tag{6}$$

in which

$$\mathscr{R}_{i_1 i_2 i_3 i_4 j_1 j_2 j_3 j_4} = R_{j_1 i_1} R_{j_2 i_2} R_{j_3 i_3} R_{j_4 i_4} \tag{7}$$

where $R_{j_k i_k}$ denote the components of the orthogonal tensor that represent the rotation of the fibre reference frame with respect to the global one, and:

$$\mathscr{T}'(a^i) = \left[1 + \mathscr{C}^{m^{-1}}(\mathscr{C}^f - \mathscr{C}^m)\,\mathscr{S}(a^i)\right]^{-1} \tag{8}$$

is the so-called stress concentration tensor in which $\mathscr{S}(a^i)$ is the Eshelby tensor of the generic inclusion. From Equations 1–3 it follows:

$$\bar{\sigma} = \left\{\mathscr{C}^m + \left[\sum_i \alpha^i(\mathscr{C}^f - \mathscr{C}^m)\,\mathscr{T}(g^i, a^i)\right] \times \left[\alpha^m 1 + \sum_i \alpha^i \mathscr{T}(g^i, a^i)\right]^{-1}\right\}\bar{\varepsilon} \tag{9}$$

where the braced member defines the elastic tensor under the Mori–Tanaka, MT, assumption (cf. Equation 1):

$$\mathscr{C}^{MT} = \mathscr{C}^m + \left[\sum_i \alpha^i(\mathscr{C}^f - \mathscr{C}^m)\,\mathscr{T}(g^i, a^i)\right] \times \left[\alpha^m 1 + \sum_i \alpha^i \mathscr{T}(g^i, a^i)\right]^{-1} \tag{10}$$

The solution of Equation 9 requires that both the orientation and the shape of every single inclusion are known. In practice, a very large number of inclusions are usually met so that the use of Equation 9 is not advisable. As a consequence it becomes necessary to consider a statistical description of the fiber orientations and aspect ratios. If $f(g)$ and $h(a)$ denote the fibre orientation density function and the aspect ratio density function, respectively, we can write

$$\sum_i \alpha^i \mathscr{T}(g^i, a^i) = \left[\sum_i \alpha^i\right] \iiint_{ES} \left[\iint_{AS} \mathscr{T}(g, a)\, h(a)\, da\right] f(g)\, dg \tag{11}$$

where ES and AS indicate the space of the Euler angles and the space of the aspect ratios, respectively. In particular:

$$\iint_{AS} \mathscr{T}_{ijkl}(g, a)\, h(a)\, da = R_{mi}(g)\, R_{nj}(g)\, R_{pk}(g)\, R_{ql}(g) \iint_{AS} \mathscr{T}'(a)\, h(a)\, da = R_{mi}(g)\, R_{nj}(g)\, R_{pk}(g)\, R_{ql}(g)\, \overset{*}{\mathscr{T}} \tag{12}$$

It follows

$$\iiint_{ES}\left[\iint_{AS} \mathscr{T}(g, a)\, h(a)\right] f(g) = \left[\iiint_{ES} \mathscr{R} f(g)\right] \overset{*}{\mathscr{T}} = \langle \mathscr{R} \rangle \overset{*}{\mathscr{T}} \tag{13}$$

If $\sum_i \alpha^i$ is denoted by α^f, the effective elastic tensor under the Mori–Tanaka assumption is:

$$\mathscr{C}^{MT} = \mathscr{C}^m + \left[\alpha^f(\mathscr{C}^f - \mathscr{C}^m)\langle \mathscr{R} \rangle \overset{*}{\mathscr{T}}\right] \times \left(\alpha^m 1 + \alpha^f \langle \mathscr{R} \rangle \overset{*}{\mathscr{T}}\right)^{-1} \tag{14}$$

an expression which is useful in the numerical evaluations.

3. Experimental procedure and results

The specimens (Fig. 1) employed in this research, were obtained by injection moulding and were composed of polybutylene terepthalate (PBT). The glass fibre reinforcement was E glass of cylindrical shape and 10 μm in diameter. The fibre weight concentration considered ranged from 0 to 47.5%. The fibres were coated with a coupling agent in order to improve the fibre–matrix bonding. The higher concentration quoted above (47.5%) was found to be an upper bound, because the aggregate was not workable in the injection procedures.

The elastic constants were evaluated with tensile tests on a standard Instron testing machine. Test control and data acquisition were provided by a microcomputer. At least five tests were performed for each condition.

The matrix was characterized by a non-linear response. The plastic range of the material appeared to be very extended, with ultimate strains greater than 100%. Between strains of 200–400 με the secant modulus is 2950 MPa, whereas between 600–2400 με

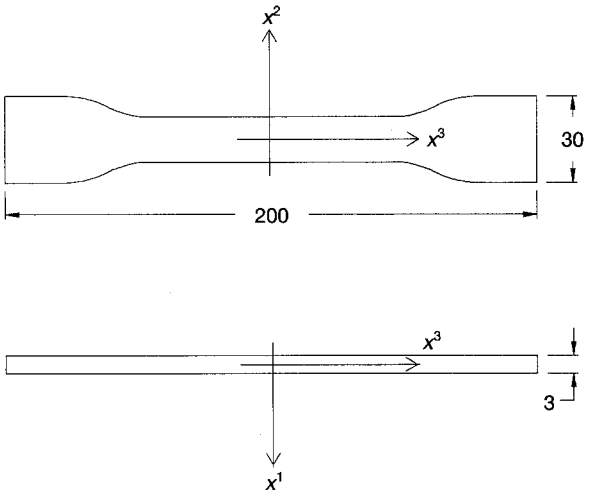

Figure 1 Test specimen.

the secant modulus becomes 2587 MPa. Poisson's ratio, evaluated in the second deformation range, is $\nu = 0.405$.

In the reinforced specimens, since the fibre length distribution was altered by the injection procedures (cf. [13]), it was necessary to measure them again. This length determination was derived semiautomatically, through an image analyser, applied to microphotographs of the ashes of specimen portions. This method requires the burning off of the polymer, and the fibre spreading onto a slide. The distributional data on the length profile are summarized in Table I.

The fibre orientation profile may be characterized by the planar angles α and β (Fig. 2); α is the angle between the projection of the principal fibre axis in the plane x_2–x_3 and the x_2 direction; and β, similarly, refers to x_1–x_3 and x_1. The determination of these angles was performed on polished sections $x_1 = 0$ and $x_2 = 0$, respectively. In all cases, an excellent alignment of the fibres with the specimen principal axis, x_3, was recorded. Table II reports the planar angle distribution for the 30 and 47.5 wt % fibre concentrations.

Two sets of experiments were performed on the reinforced specimens:

1. standard tensile tests in the specimen principal direction, x_3; and
2. tensile tests in one transverse direction, x_2.

In the former case, the longitudinal Young's modulus, E_3, was determined, whereas in the latter tests the transverse Young's modulus, E_2, and the Poisson's ratio, ν_{32}, were measured. Due to the specimen shape (exiguous length in the x_2-direction), the second tests were performed on specimens prepared as schematically sketched in Fig. 3.

As stated, the considered matrix (PBT) is characterized by non-linear behaviour. However, the composite shows an almost linear response in the longitudinal direction, corresponding to the maximum fibre alignment. Conversely, the transversal response is non-linear, qualitatively similar to the matrix response. The secant longitudinal Young's modulus, E_3, measured between strains of 600–2400 $\mu\varepsilon$, the transverse Young's modulus, E_2, and the Poisson's ratio, ν_{32}, measured between strains of 200–400 $\mu\varepsilon$ are reported in Table III. The lower strain range was considered in order to avoid possible inelastic phenomena in the glued sections that would have conditioned the stress field in the experiments.

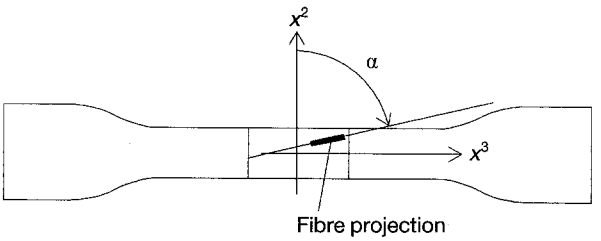

Figure 2 Planar angle, α, of the generic fibre.

TABLE I Distributional data on the length profile

Length classes (μm)	Relative frequency for fibre concentrations spanned		
	10 wt %	20 wt %	40 wt %
0–50	0.000	0.000	0.000
50–100	0.515	0.468	0.416
100–180	0.144	0.167	0.252
180–260	0.054	0.134	0.150
260–340	0.044	0.074	0.094
340–420	0.035	0.050	0.058
420–500	0.042	0.037	0.017
500–590	0.022	0.027	0.004
590–680	0.033	0.010	0.004
680–780	0.025	0.010	0.004
780–890	0.019	0.003	0.000
890–4000	0.067	0.020	0.001

TABLE II Planar angle distributions for 30 and 47.5 wt % fibre concentrations

Angle	For 30 wt % conc.		For 47.5 wt % conc.	
	f_α	f_β	f_α	f_β
175	0.0000	0.0000	0.0086	0.0000
165	0.0127	0.0112	0.0029	0.0000
155	0.0127	0.0056	0.0029	0.0000
145	0.0000	0.0225	0.0057	0.0109
135	0.0127	0.0281	0.0258	0.0328
125	0.0253	0.0281	0.0344	0.0109
115	0.0886	0.0843	0.0745	0.0929
105	0.1643	0.1124	0.1289	0.1475
95	0.2532	0.1685	0.2687	0.2623
85	0.2152	0.2528	0.3324	0.2951
75	0.1013	0.1011	0.0458	0.0492
65	0.0380	0.0843	0.0315	0.0273
55	0.0253	0.0506	0.0086	0.0328
45	0.0253	0.0112	0.0057	0.0000
35	0.0127	0.0169	0.0143	0.0164
25	0.0127	0.0112	0.0115	0.0055
15	0.0000	0.0056	0.0029	0.0189
5	0.0000	0.0056	0.0029	0.0055

4. Discussion

In order to compare the experimental results with the forecasts expressed by the Mori–Tanaka approximation, the microstructural characterization presented in Section 3 was used.

TABLE III

	Concentration (wt %)				
	10	20	30	40	47.5
Longitudinal modulus (MPa)	4270	6550	9250	12310	14840
Standard deviation (%)	6.05	3.55	2.86	1.69	2.33
Transverse modulus (MPa)	3363	3828	4378	5075	5931
Standard deviation (%)	4.12	1.54	1.55	2.45	1.77
Poisson's ratio (ν_{32})	0.31	0.24	0.19	0.16	0.14
Standard deviation (%)	3.54	3.57	2.12	4.91	0.71

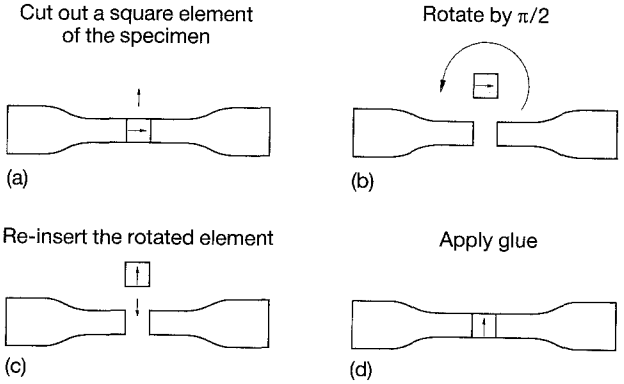

Figure 3 Specimens used in tensile tests in one transverse direction.

TABLE IV Least square method of evaluation of experimental data

Concentration (wt %)	A	B	σ_1	σ_2
30	0.2158	0.0104	0.0657	2.1773
50	0.3100	0.0127	0.0293	4.3206

The numerical evaluation requires an orientation density function (ODF). Since the planar angles α and β are close approximated by the same distribution, transverse isotropy was assumed. In other words, it was supposed that on every plane containing the x_3 axis there was an equal planar angle distribution. On the basis of the experimental data, the following planar density function $\Gamma(\Phi)$ was considered:

$$\Gamma(\Phi) = A\exp\frac{-(\Phi - \pi/2)^2}{2\sigma_1} + B\exp|(\Phi - \pi/2)/(2\sigma_2)| \quad (15)$$

where A, B, σ_1 and σ_2 have been evaluated with the least square method applied to the experimental data reported in Table IV.

The ODF in the Mori–Tanaka scheme is expressed in terms of the so-called Euler angles φ_1, Φ and φ_2 defined according to Fig. 4. The fixed reference frame $\{e^1\}$ is assumed to coincide with the specimen axes, and $\overset{*}{e}{}^2$ axis of the frame adherent to the generic fibre is taken as parallel to the principal fibre axis. It may be shown that the ODF corresponding to the assumed planar angle is:

$$f(\varphi_1, \Phi, \varphi_2) = f_1(\varphi_1) f_0(\Phi) f_2(\varphi_2) \quad (16)$$

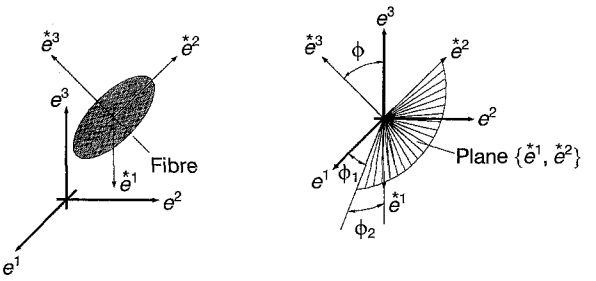

Figure 4 Euler angles φ_1, Φ and φ_2.

where $f_1(\varphi_1)$ is a constant, $f_2(\varphi_2) = \delta(0)$, (Dirac's δ) and:

$$f_0(\Phi) = \Gamma(\Phi) = A\exp\frac{-(\Phi - \pi/2)^2}{2\sigma_1} + B\exp|(\Phi - \pi/2)/(2\sigma_2)| \quad (17)$$

With regard to the aspect ratio distribution to be used in the Mori–Tanaka model, we consider the discrete distribution obtained experimentally (values in Table I divided by the fibre diameter). For a considered fibre concentration the closest available ODF and the aspect ratio distribution were used.

Table V summarizes the numerical estimate of the five engineering elastic constants characterizing the material, together with experimental error measurements. The comparison is also illustrated in Figs 5–7, which underline a noticeable degree of agreement between theory and tests. It can be said that the model gives a realistic and acceptable assessment of the composite's behaviour over a wide range of fibre concentration. Other theoretical or semi-empirical models are not always of easy application, or cannot be employed in non-trivial fibre distribution. The numerical estimates are very sensitive to the microstructural data, and it is possible to observe that only with correct information on the material, does the model here considered give a realistic and accurate prediction of the mechanical properties. For instance, numerical evaluations assuming a fibre length equal to average fibre length, exhibit an overestimation of the effective elastic moduli.

Finally, it may be remarked that the errors incurred in measuring the transverse modulus are very small, and lower than those regarding the longitudinal modulus. In both cases, the errors are comparable to the standard deviation of the experiments.

TABLE V Experimentally determined discrete aspect ratio distribution

	Concentration (wt %)				
	10	20	30	40	47.5
Longitudinal modulus (MPa)	4368	6450	8927	12185	15311
Error (%)	2.3	− 1.5	− 3.5	− 1.05	3.2
Transverse modulus (MPa)	3424	3910	4472	5175	5843
Error (%)	1.8	2.1	2.1	2.0	− 1.5
Poisson's ratio (ν_{32})	0.286	0.222	0.183	0.152	0.126
Error (%)	− 7.7	− 7.5	− 3.7	− 5.0	− 10.0
Shear modulus G_{12} (MPa)	1015	1132	1281	1474	1665
Shear modulus G_{13} (MPa)	1076	1266	1508	1770	2000

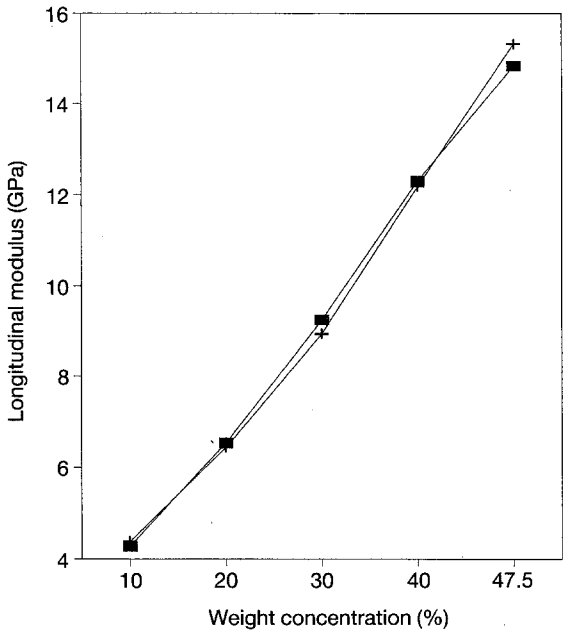

Figure 5 Effect of glass fibre concentration on the longitudinal elastic modulus: –■–, experimental; –╫–, Mori–Tanaka.

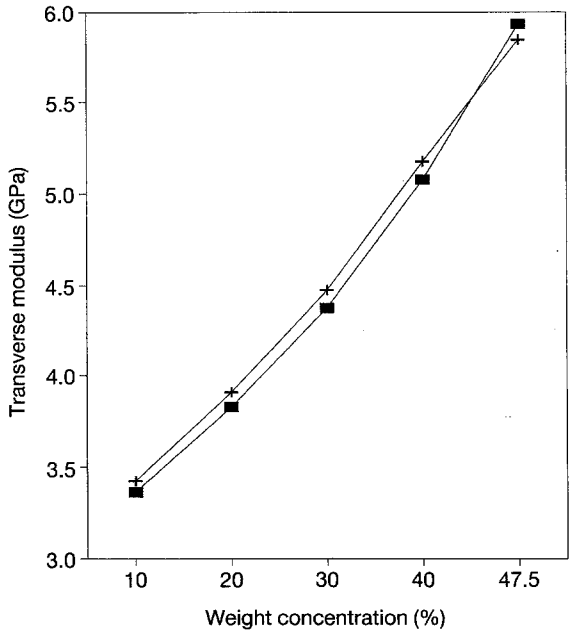

Figure 6 Effect of glass fibre concentration on the transverse elastic modulus: –■–, experimental; –╫–, Mori–Tanaka.

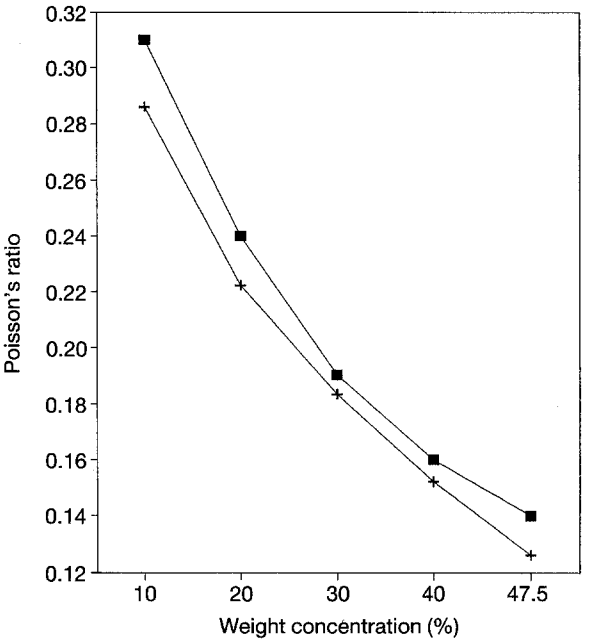

Figure 7 Effect of glass fibre concentration on the Poisson's ratio, ν_{32}: –■–, experimental; –╫–, Mori–Tanaka.

5. Conclusions

The Mori–Tanaka theory coupled with accurate microstructural characterization gives an excellent estimate of the overall elastic properties for short fibre biphase reinforced composites. This holds true for the fibre concentration here considered, which falls within the range characteristic of the usual industrial applications. In comparison to alternative homogenization schemes, an important advantage of this model is its versatility in incorporating most general micromorphological information, independently of the fibre aspect ratios and orientational distributions.

Acknowledgements

Microstructural characterization was carried out at the Centro Ricerche Montedipe by A. Boscolo. Partial support of the Italian MURST is gratefully acknowledged.

References

1. I. K. PARTRIDGE (Ed.), "Advanced composites" (Elsevier Applied Science, London, 1989) p. 345.

2. J. D. ESHELBY, *Proc. R. Soc. Lond.* **A241** (1957) 376.
3. B. BUDIANSKY, *J. Mech. Phys. Solids* **13** (1965) 223.
4. R. HILL, *ibid.* **13** (1965) 189.
5. J. C. HALPIN and J. L. KARDOS, *Polymer Eng. Sci.* **16** (1976) 344.
6. R. McLAUGHLIN, *Int. J. Eng. Sci.* **15** (1974) 237.
7. T. MORI and K. TANAKA, *Acta Metal.* **21** (1973) 571.
8. Z. HASHIN, *J. Appl. Mech.* **50** (1983) 481.
9. R. M. CHRISTENSEN, *J. Mech. Phys. Solids* **38** (1990) 379.
10. *Idem.*, "Mechanics of composite materials" (Wiley Interscience, New York, 1979) p. 123.
11. Y. BENVENISTE, *Mech. Mater.* **6** (1987) 147.
12. M. FERRARI and G. C. JOHNSON, *ibid.* **8** (1989) 67.
13. A. BOSCOLO BOSCOLETTO, M. FERRARI, I. PITACCO and H. P. VIRGOLINI, in Proceedings of the European Mechanics Colloquium 269 'Exp. Identification of Mech. Characteristics of Composite Materials, Saint-Etienne, December 1990, edited by A. Vautrin and H. Sol (Elsevier, Norwich) p. 238.

Received 4 September 1992
and accepted 27 September 1993